

ON DESIGN AND ANALYSIS OF A HIGH BRIGHTNESS ELECTRON SOURCE*

Zohreh Parsa
Brookhaven National Laboratory

and

Lloyd Young
Los Alamos National Laboratory

Abstract

Developments of the high brightness sources have led to new advances in the accelerator technology, and new experimental programs, such as FEL or IFEL experiments. We present a brief overview, discuss the Brookhaven photocathode gun, and illustrate some of our analysis results. We also note the effects of the rf and space charge forces (and their correlations) on the beam.

Introduction

The high brightness laser-driven radio frequency (rf) guns are potential sources of high current, low emittance and short bunch beams of electrons, required for the future development of linear colliders, and new methods of acceleration, such as free electron lasers (FEL), and inverse free electron lasers (IFEL).

Such a gun consists of an rf cavity with a photocathode surface placed at its end wall, a high power laser beam that illuminates the cathode, where the emitted electrons are accelerated immediately by a strong rf field (in the cavity) to a relativistic energy. The beam is controlled by the laser, thus eliminating the need for bunchers, and allowing the electric field (in the rf cavities) to be very strong to minimize the (degrading) space charge effects on the beam. The design of such guns originated at LANL and is being developed and used at other facilities, e.g., at Brookhaven National Laboratory (BNL), discussed in the next section.

Brookhaven ATF Photocathode Gun

To achieve high brightness and rapid acceleration, a radio-frequency (rf) gun operating at 2.856 GHz, with 1-1/2 cell, pi-mode, resonant, disc loaded structure (with cathode placed at the start of the 1/2 cell), is designed as the injector for the BNL Accelerator Test Facility (ATF). ATF consists of a 50 to 100 MeV electron beam of about 6 psec pulse length, which is synchronized with a (100 GW peak power) CO₂ laser used to excite an open end accelerating structure. The gun and accelerating systems are initially driven by a single 30 MW Klystron, to produce a 50 MeV beam, to be upgraded (later) with a 2nd Klystron to the output energy of about 100 MeV [1]. Further, experiments require the photocathode with a picosecond response time, low emittance, mechanical stability and good quantum efficiency. Hence, initially, an Yttrium (with work function of -3.1 eV) cathode will be used, and illuminated by either a frequency-quadrupled or tripled Nd:Yag laser, depending on the experimental requirements. E.g., the Nd:Yag laser pulse will be shaped and used to initiate the CO₂ laser pulse (discussed above), allowing for a class of CO₂-laser-electron beam coincidence experiments. In Table I, some of the rf gun design parameters are given, and in the next section some results of our analysis are presented.

Table I. Gun Design Parameters

Number of Cells	1-1/2
Lengths (cm):	
1st (1/2) cell	2.625
2nd cell	5.25
structure length	7.875
structure inner diameter	8.308
Operating Frequency (MHz)	2856

Analysis and Emittance Calculation

The results obtained for initial average axial electric fields of $E_0 = 66.6$ MV/m (design value), and $E_0 = 63.75$ MV/m (test value, produces the proposed beam of 4.5 MeV/c at the gun exit, with Program PARMELA [2]), are presented. With a Gaussian distribution of (1000) particles, placed behind the cathode (no acceleration), with initial phase of 59° (and 65° on the cathode), and initial size of $\sigma_r = 0.3$ cm and $\sigma_z = 2.06^\circ$ (2 psec = 2.06°), the calculated beam parameters (at every 10° phase through the gun are given in Table III with $E_0 = 66.6$ MV/m). For $E_0 = 63.75$ MV/m, the beam parameters were calculated from the cathode through the transport beam line to the (element 27) LINAC entrance, and are illustrated in Table II. For more information see [3] and [4]. In these tables, the element names (ne, e.g., ne = 1,2,3 corresponds to "cathode", "1st (1/2) cell", and "2nd cell" respectively), number of particles (np), calculated beam energy (w), and beam emittance ("rms" and "90%"), are included.

Figure 1 shows the schematic of the electron gun. Figures 2 and 3 show the beam profiles and phase plots of the parameters at the gun exit (element 3) for the two cases with $E_0 = 63.75$ MV/m (average axial electric fields) and $E_0 = 66.6$ MV/m, respectively.

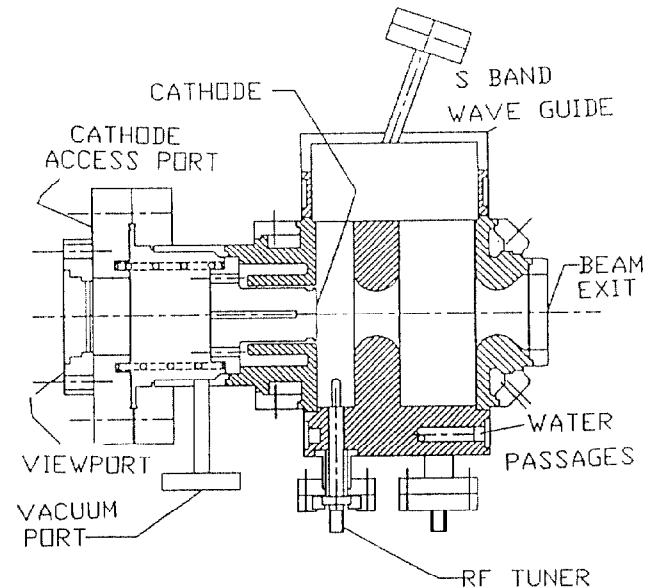
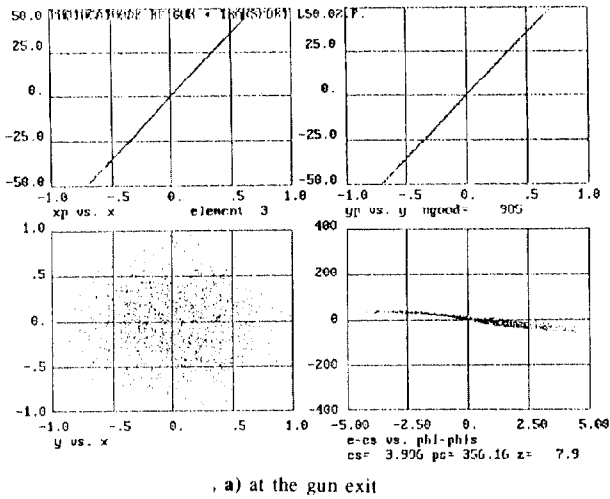


Fig. 1. Schematic of BNL-Photocathode e Gun

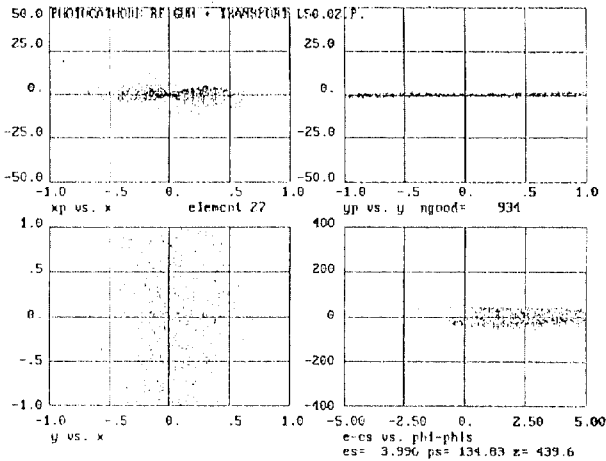
In Table IV, a summary of our results for the two cases is given for comparison with previous calculations, e.g., [1]. The fields were calculated with Program Superfish [7], from which we calculated the shunt impedance (Z_{II}), transient time factor (τ_0^0) and $Z_{II} = Z_{II}^0$ given below, (For more details see Ref. [4]):

element	length (cm)	Z_{II} (Mohm/m)	Y_0	Z_{II}^0 (Mohm/m)
1st (1/2) cell	2.625	46.22	0.8461	33.08
2nd cell	5.25	72.49	0.7709	43.082
total cavity	7.875	63.74	0.7967	40.46

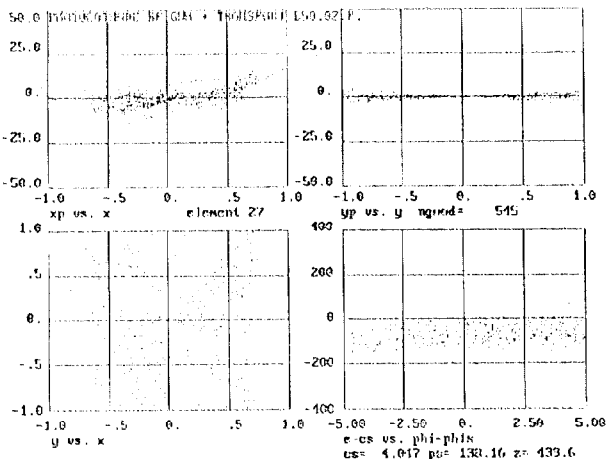
*Work performed under the auspices of the U.S. Department of Energy



a) at the gun exit



b) at the LINAC Entrance (element 27) with space charge turned off (934/1000 part. survived),



c) with space charge turned on (545/1000 particles survived).

Fig. 2. Beam profiles for the case $E_0 = 63.75$ MV/m, a) at the gun exit (element 3), b) at the LINAC Entrance (element 27) with space charge turned off (934/1000 part. survived), c) with space charge turned on (545/1000 particles survived).

Table II. ATF-Photocathode rf Gun and Transport Line Parameters Calculated with PARMELA (with initial average axial electric field $E_0 = 63.75$ MV/m); emittance is given in (π cm-mrad) with s.c. off in transport line.

nel no.	z1 (cm)	element name	rms, n x	emax, n x, 90%	rms, n y	emax, n y, 90%
1	0.0	drift	0.0192	0.0988	0.0185	0.0921
2	0.0	cell	0.9543	3.9990	0.9935	4.1602
3	2.6	cell	1.2067	5.1348	1.2300	5.1948
4	7.9	drift	1.2446	5.2598	1.2745	5.3789
5	10.1	quad	3.4725	14.1250	1.4883	6.2258
6	22.2	drift	3.5598	14.8750	1.4918	6.2402
7	22.8	quad	7.1480	26.8203	1.3553	5.5645
8	43.6	drift	7.1894	27.0156	1.3628	5.5889
9	44.2	quad	5.7934	25.6169	1.5120	6.4019
10	56.3	drift	6.1091	27.6493	1.5618	6.5975
11	112.1	bend	10.7122	49.8750	1.8197	7.4761
12	132.1	drift	10.7047	49.7177	1.8222	7.4899
13	152.3	quad	10.7050	49.7080	1.8217	7.4849
14	164.3	drift	10.7101	49.7942	1.8206	7.4808
15	179.0	drift	10.7151	49.8803	1.8195	7.4801
16	193.7	quad	10.7137	49.9063	1.8201	7.5142
17	205.8	drift	10.6987	49.8165	1.8247	7.5996
18	226.0	bend	6.4219	29.1643	3.7595	16.0112
19	246.0	drift	6.4449	29.1093	3.8590	16.6719
20	273.8	quad	6.3899	29.5938	4.1987	18.7500
21	288.2	drift	6.3952	29.4583	4.2384	18.7656
22	288.8	quad	5.9303	27.2109	5.3904	25.4717
23	312.2	drift	5.9336	27.2461	5.4313	25.6670
24	312.8	quad	5.7361	27.1116	5.8265	27.7560
25	327.2	drift	5.7269	27.0847	5.8260	27.7585
26	388.4	drift	5.7239	27.0757	5.8258	27.7593
27	408.6	drift	5.7194	27.0620	5.8255	27.7606

Table III. Gun Parameters Calculated with $E_0 = 66.6$ MV/m (Design Value) Units of Phase in Degrees, Energy w_r in MeV, rms emittance e_x or e_y in π cm-mrad

ne	np	ref phase	z_r (cm)	w_r	e_x^{rms}	e_y^{rms}
0	1000	69.0	0.0	0.011		
1	1000	65.2	0.0	0.000	.0144	.0158
0	1000	79.0	0.1	0.128		
0	1000	89.0	0.4	0.332		
0	1000	99.0	0.6	0.572		
0	1000	109.0	0.9	0.811		
0	1000	119.0	1.1	1.030		
0	1000	129.0	1.4	1.211		
0	1000	139.0	1.7	1.345		
0	1000	149.0	2.0	1.430		
0	1000	159.0	2.3	1.473		
0	999	169.0	2.5	1.485		
0	998	179.0	2.8	1.485		
2	998	172.1	2.6	1.486	.8891	.9148
0	998	189.0	3.1	1.490		
0	995	199.0	3.4	1.515		
0	994	209.0	3.7	1.578		
0	991	219.0	3.9	1.688		
0	989	229.0	4.2	1.848		
0	989	239.0	4.5	2.055		
0	989	249.0	4.8	2.300		
0	989	259.0	5.1	2.572		
0	989	269.0	5.4	2.857		
0	989	279.0	5.7	3.142		
0	989	289.0	6.0	3.413		
0	989	299.0	6.2	3.655		
0	989	309.0	6.5	3.856		
0	989	319.0	6.8	4.008		
0	989	329.0	7.1	4.107		
0	989	339.0	7.4	4.159		
0	989	349.0	7.7	4.177		
0	989	359.0	8.0	4.179		
3	989	355.2	7.9	4.179	1.1523	1.1354
0	989	369.0	8.3	4.179		
0	989	379.0	8.6	4.179		
0	989	389.0	8.9	4.179		

Appendix

On rf Field and Space Charge Contributions

The increase in the beam emittance due to radio frequency (rf) field comes from the time variation of transverse forces, as seen by various electrons. For example, for an electron beam (with a Gaussian density distribution $\rho(x, y, \Delta z)$, and lengths σ_x, σ_z), emittance may be estimated by:

$$a. 1 \quad e_x^{rf} = \frac{a}{\sqrt{2}} k^3 \sigma_x^2 \sigma_z^2, \quad e_z^{rf} = \sqrt{3} (\gamma_f - 1) k^2 \sigma_z^3$$

where $a \equiv eE_0/2mc^2k$ is dimensionless rf strength.

With

$$\rho(x, y, \Delta z) \equiv \rho_0 e^{-1/2 \left[\frac{x^2 + y^2}{\sigma_x^2} + \frac{\Delta z^2}{\sigma_z^2} \right]},$$

the space charge (sc) induced emittance (transverse (x) and longitudinal (z)) may be estimated by

$$e_x^{sc} \text{ (or } z) = \pi I C_x \text{ (or } z) (\sigma_x / \sigma_z) / 4akl_A \sin \phi_0$$

where I is the peak current, $I_A = 4\pi\epsilon_0(mc^3/e) = 17,000 \text{ A}^\circ$ (known as Alfren current), ϕ is the rf phase at the cavity exit and C_x (or z) (σ_x / σ_z) are defined as dimensionless, transverse and longitudinal space charge factor(s) that depend on the given distribution.

Although the space charge and rf contributions are treated separately in most calculations (e.g., above), the correlation between these two effects should be noted, as the total emittance cannot be separated into two parts. For example, given the total momentum $p_x = p_x^{rf} + p_x^{sc}$, the total emittance becomes:

$$e_x = \sqrt{(e_x^{rf})^2 + (e_x^{sc})^2 + 2(e_x^{rf})(e_x^{sc}) J_x}$$

with the correlation function,

$$J_x \equiv \frac{1}{e_x^{rf} e_x^{sc}} \left[\langle x^2 \rangle \langle p_x^{rf} p_x^{sc} \rangle - \langle x p_x^{rf} \rangle \langle x p_x^{sc} \rangle \right]$$

e.g., $-1 < J_x < 1$, for a Gaussian distribution [5], which is not negligible. For more accuracy one may include the higher order moments and their correlations in the emittance formulation, e.g., see [3], [6].

References

- [1] K. Batchelor et al., Proceedings of Acc. Physics Confs., Williamsburg, Va (1988), AIP Part. Acc. Conf., Chicago, Ill. (1989), Proceedings of EPAC, Rome (1988).
- [2] L. Young, author of program PARMELA. We note our results differ from those obtained earlier with modified and/or older versions of this program, e.g., Ref. [1].
- [3] Z. Parsa, On ATF-Photocathode rf Gun, CAP Note 7, (12/6/90) and BNL Report (1990); On Re-evaluation of ATF-Photocathode rf Gun and the Transport Beamline, CAP Note 8 (2/13/90) and BNL Report (1990).
- [4] Z. Parsa and L. Young, High Brightness Photocathode Injector for BNL Accelerator Test Facility, BNL Report (1990).
- [5] Kim, K.J., Lawrence Berkeley Lab Report, LBL-25807 (1988).
- [6] Z. Parsa, On Beam Emittance and Invariants...., This procedgs.
- [7] SUPERFISH, Ref. Manual La-ur-87-126, LANL.
- [8] Z. Parsa, D. Choudhury, Linear and NonLinear analysis of the Brookhaven ATF Transport Beamline ADD/CAP/TN 14, (7/27/89).

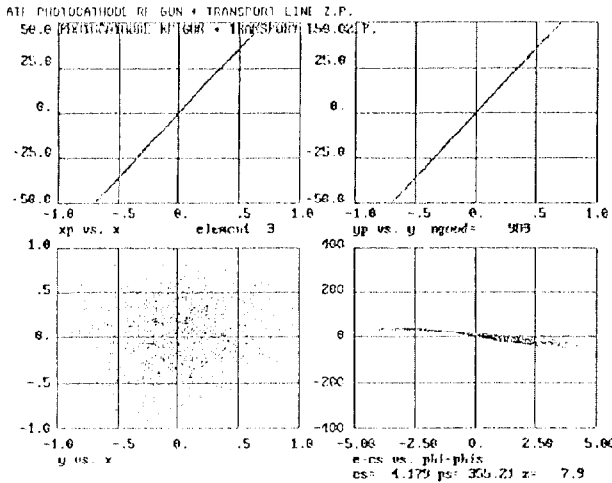


Fig. 3. Phase space plots of the beam parameters at the gun exit (element 3) for the case of $E_0 = 66.6 \text{ MV/m}$ (initial average axial electric field), where 989/1000 particles survived, with kinetic energy of 4.179 MeV at the end of the (2-1/2 cell) cavity of 7.9 cm length.

Table IV. Summary of Beam Parameters at the Gun Exit

E_0 (MV/m)	E_{cathode} (MV/m)	w_r (MeV)	p (MeV/c)	emittance ($\pi\text{cm-mrad}$) rms	
				e_x	e_y
66.6	100.03	4.17	4.653	1.15	1.14
63.75	95.75	3.996	4.478	1.21	1.23

E_0 = average axial electric field.

E_{cathode} = corresponding field on the cathode.

w_r = kinetic energy.

p = corresponding momentum.

Summary

Laser-driven radio frequency guns are the potential sources for high current low emittance beam required for new methods of accelerations such as IFEL. We illustrated some of our analysis for the Brookhaven ATF-photocathode and transport beamline with program PARMELA [2]. The field calculations were made with program SUPERFISH, from which shunt impedance and transient time factors were calculated and tabulated. Table IV, shows the beam emittance calculated at the Gun exit, to be $\sim 12 \pi\text{-mm-mrad}$ as compared to $\sim 7 \pi\text{-mm-mrad}$ obtained in the earlier calculations [1], with other (older and/or modified) versions of PARMELA (and SUPERFISH). Fig 3, show the beam profile at the gun exit and at LINAC entrance, (with space charge turned off (Table II), and on (see [3]), in the Transport line), respectively. Our results with PARMELA, for the beamline, confirms the earlier findings with Lie Algebraic method [8], that the beam diverges too much, gets large and leads to emittance growth. Some of the possible solutions [3,4] were, an overall improvement in the gun performance and placing of the gun directly to the LINAC entrance e.g. use of solenoids, or changing the shape of the cathode wall so as to obtain some focussing in the 1st cell which produce some additional focussing in the 2nd cell, etc. [3].